

See discussions, stats, and author profiles for this publication at: <https://www.researchgate.net/publication/14521352>

# Conformational Constraints on the Headgroup and sn -2 Chain of Bilayer DMPC from NMR Dipolar Couplings †

ARTICLE *in* BIOCHEMISTRY · JULY 1996

Impact Factor: 3.02 · DOI: 10.1021/bi953083i · Source: PubMed

CITATIONS

44

READS

22

## 3 AUTHORS:



**Mei Hong**

Iowa State University

152 PUBLICATIONS 6,239 CITATIONS

SEE PROFILE



**Klaus Schmidt-Rohr**

Brandeis University

249 PUBLICATIONS 8,968 CITATIONS

SEE PROFILE



**Herbert Zimmermann**

Max Planck Institute for Medical Research

305 PUBLICATIONS 5,500 CITATIONS

SEE PROFILE

# Conformational Constraints on the Headgroup and *sn*-2 Chain of Bilayer DMPC from NMR Dipolar Couplings<sup>†</sup>

M. Hong\*

Materials Sciences Division, Lawrence Berkeley National Laboratory, 1 Cyclotron Road, and Department of Chemistry, University of California, Berkeley, California 94720

K. Schmidt-Rohr

Department of Polymer Science and Engineering, University of Massachusetts, Amherst, Massachusetts 01003

H. Zimmermann

MPI für Medizinische Forschung, Arbeitsgruppe Molekulkristalle, Jahnstrasse 29, D-69120 Heidelberg, Germany

Received December 29, 1995; Revised Manuscript Received February 23, 1996<sup>®</sup>

**ABSTRACT:** This paper presents new NMR constraints on the conformation of the headgroup, glycerol backbone, and *sn*-2 chain of 1,2-dimyristoyl-*sn*-glycero-3-phosphatidylcholine (DMPC) in the liquid-crystalline bilayer. Using two-dimensional <sup>13</sup>C–<sup>1</sup>H chemical shift correlation spectroscopy, we find significant dipolar couplings between the carboxyl carbon CO<sub>2</sub> and the headgroup protons. This indicates that a conformation in which the DMPC headgroup and the beginning of the *sn*-2 chain bend toward each other is significantly populated in the fluid bilayer. The predominance of this headgroup orientation can be further confirmed by <sup>31</sup>P–<sup>13</sup>C dipolar couplings from the literature, which constrain the glycerol G2–G3 torsion angle to be close to *trans*, excluding a significant presence of one of the two conformations found in the DMPC crystal. Combining and reexamining 20 known NMR couplings for the glycerol backbone and its adjacent segments of L<sub>α</sub>-DMPC, we find that several torsion angles and bond orientations in the core of the DMPC molecule are constrained severely and must differ from those in the crystal structure. We propose a consistent molecular model for phosphocholine lipids in the liquid-crystalline phase, with a rigid backbone in the core of the molecule, a bent-back headgroup, and increasing mobility toward the ends of the acyl chains and the headgroup.

Phospholipids are the basic structural components of biological membranes, which are essential in compartmenting the fluid biological phases of all organisms. They play an important role in membrane functions such as material transport, cell–cell recognition, and signal transduction (Petty, 1993; Silver, 1985; Lehninger et al., 1993). Thus, a detailed knowledge of the molecular structure of the phospholipids is necessary for understanding bilayer membranes and the interactions of the lipids with other membrane constituents such as proteins and sterols. However, due to the liquid-crystalline nature of the lipid bilayers, the molecular conformations of the phospholipid molecules have proven to be difficult to characterize, even by powerful scattering and spectroscopic techniques. The clearest structural result was obtained from neutron scattering studies on phosphatidylcholine, which showed a bend of the headgroup at the phosphate junction (Büldt et al., 1978). Such a bend causes the headgroup's O–C $\alpha$ –C $\beta$ –N backbone to be nearly parallel to the bilayer surface. This bend has been corroborated by NMR measurements of C–H bond order parameters, which change sign at the phosphate junction (Hong et al., 1995b), and which indicate that the C–H bonds

of the glycerol G3 site are preferentially oriented at angles larger than 50° from the director (Schmidt-Rohr & Hong, 1995).

While the bend of the headgroup with respect to the glycerol backbone is quite well documented, the orientation of the headgroup (and its dynamics) with respect to the junction of the glycerol G2 segment and its attached acyl chain has not been elucidated. The relative orientation of the headgroup with the plane containing the two acyl chains is important for determining the effective shape of the molecule. Two conformations with different headgroup orientations are manifested in the X-ray crystal structure of 1,2-dimyristoyl-*sn*-glycero-3-phosphatidylcholine (DMPC) at low hydration levels (Figure 1) (Pearson & Pascher, 1979). Conformation A shows the headgroup pointing away from the rest of the molecule, while the headgroup in conformation B is folded back, resulting in a more compact structure. However, due to crystal packing effects, the degree of similarity between the molecular conformations in the crystal and in the liquid-crystalline bilayers is uncertain and must be tested experimentally. For example, major conformational differences are known to exist in the fatty acid chains: they are all-*trans* in the gel and crystalline phases but are highly flexible in the liquid-crystalline state.

A related question concerns the degrees of freedom of the phospholipid molecule in the liquid-crystalline state. Simple

<sup>†</sup> M.H. is supported by the Director, Office of Energy Research, Office of Basic Energy Sciences, Materials Sciences Division of the U.S. Department of Energy, under Contract DE-AC03-76SF00098.

<sup>®</sup> Abstract published in *Advance ACS Abstracts*, June 1, 1996.

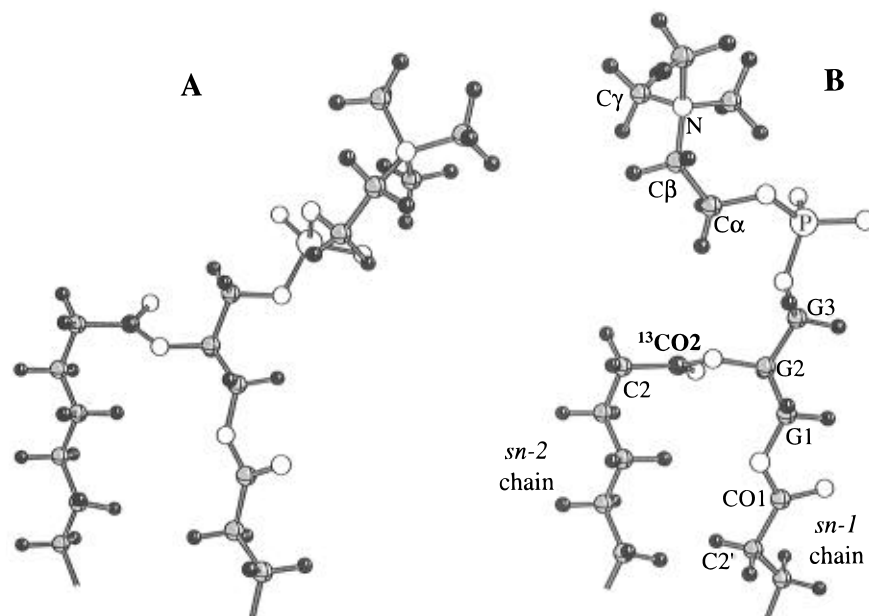


FIGURE 1: Two molecular conformations A and B in the unit cell of DMPC crystals, as determined by X-ray scattering (Pearson & Pascher, 1979). The headgroup points away from the two acyl chains in molecule A, while it hangs closely above the *sn*-2 chain in molecule B. The different headgroup orientations mainly result from the difference in the torsion angle G1–G2–G3–O in the glycerol backbone region. This torsion is gauche<sup>+</sup> for molecule A and trans for molecule B (Pearson & Pascher, 1979). The nomenclature used in the text is indicated on molecule B. The *sn*-2 chain carboxyl carbon CO2 is isotopically enriched in the current experiments.

models derived from the crystal structure implicitly assume strong conformational restrictions. On the other hand, <sup>2</sup>H quadrupolar splittings (Seelig et al., 1977; Skarjune & Oldfield, 1979) and <sup>1</sup>H–<sup>1</sup>H dipolar couplings (Hong et al., 1995a) verified that exchange between at least two conformations occurs in the headgroup of phosphocholine lipids, and demonstrated increasing mobilities toward the end of the acyl chains (Seelig & Seelig, 1980). Meanwhile, molecular dynamics and Monte Carlo simulations suggest that all parts of the molecule are very flexible, with a large range for various torsion angles (Stouch, 1993; Konstant et al., 1994). Such an extreme structural flexibility is possible, at least in a single-molecule picture, if one considers that most bonds in phosphocholine are single bonds and no rings are present to make the structure more rigid. Therefore, one might question whether it is possible to approximate any part of the phospholipid in the liquid-crystalline state by a single conformation.

In this paper, we explore the conformations of L-α-phosphocholine at the headgroup and the junction of the *sn*-2 chain and the glycerol backbone, using synthetic <sup>13</sup>CO<sub>2</sub>-labeled DMPC as a model system. We report the estimation of the relative strengths of long-range <sup>13</sup>C–<sup>1</sup>H dipolar couplings by two-dimensional (2D) solid-state NMR techniques. Our first goal is to determine the headgroup orientation relative to other parts of the molecule, specifically, the acyl chains. This cannot be achieved by measurements of short-range, segmental NMR couplings or of the headgroup P–N vector orientation relative to the bilayer normal, since the headgroups in the two proposed conformations by <sup>2</sup>H NMR (Seelig et al., 1977) are related by approximate inversion of their torsion angles and have nearly the same orientation with respect to the bilayer normal. However, the long-range dipolar couplings between the acyl chain and the headgroup can establish significant constraints on the conformation of the DMPC headgroup. With these structural considerations, we come to a second objective: to determine

whether the NMR data for the glycerol backbone and the adjacent segments reported in the literature are consistent with a single-conformation model for the core of the phosphocholine molecule.

## MATERIALS AND METHODS

**Synthesis:** 1-Myristoyl-2-[1-<sup>13</sup>C]myristoyl-*sn*-glycero-3-phosphatidylcholine. [1-<sup>13</sup>C]Myristic acid (<sup>13</sup>C = 99%) was prepared by low-temperature carboxylation (–30 °C) of the tridecylbromide-Grignard in ether with <sup>13</sup>CO<sub>2</sub>. The corresponding labeled anhydride was prepared via [1-<sup>13</sup>C]myristic acid by the use of dicyclohexylcarbodiimide (Salinger & Lapidot, 1966). Subsequently, 1-myristoyl-2-[1-<sup>13</sup>C]myristoyl-*sn*-glycero-3-phosphatidylcholine was synthesized by esterification (Radhakrishnan et al., 1981; Hermetter & Paltauf, 1981) of 1-myristoyl-2-hydroxy-*sn*-glycero-3-phosphocholine (Avanti Polar Lipids, Inc.) with the labeled myristic anhydride and dimethylaminopyridine in CHCl<sub>3</sub>. The reaction was monitored with TLC until the 2-lysophosphatidylcholine had disappeared. The product was purified by chromatography on Sephadex LH-20 with CHCl<sub>3</sub> as eluent. Most of the solvent evaporated at room temperature, and the labeled dimyristoylphosphatidylcholine was precipitated with ether. Repeated recrystallizations from CHCl<sub>3</sub>/ether resulted in a white crystalline product (one spot on TLC = CHCl<sub>3</sub>/CH<sub>3</sub>OH/H<sub>2</sub>O = 65:25:10; iodine).

**Sample Preparation.** The resulting dry DMPC powder was hydrated with D<sub>2</sub>O at a 50:50 (w/w) ratio, mixed, and freeze-thawed with liquid nitrogen until a uniform aqueous dispersion was formed. The hydrated powder sample was used in all experiments.

The chemical structure and the nomenclature of the various segments of DMPC are shown in Figure 1, where the <sup>13</sup>C-enriched carboxyl group on the *sn*-2 chain is highlighted.

**NMR Measurements.** The NMR experiments were conducted on a home-built 7.07-T spectrometer interfaced with

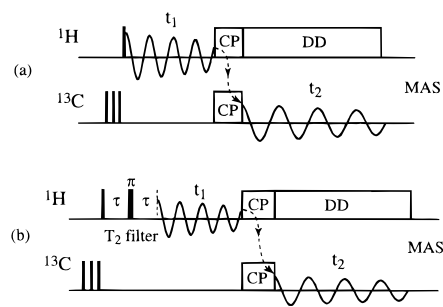


FIGURE 2: Pulse sequences used in this work. (a)  $^{13}\text{C}$  and  $^1\text{H}$  heteronuclear correlation (HETCOR) under magic-angle sample spinning. During the evolution period  $t_1$ , proton magnetization, flipped to the transverse plane by a  $90^\circ$  pulse, evolves under the chemical shift and heteronuclear (C–H) scalar interactions. At the end of  $t_1$ , the proton magnetization is transferred to carbon spins by cross polarization; then the carbon isotropic chemical shift is detected under proton decoupling. (b) A proton  $T_2$  filter is inserted before the evolution period in the HETCOR experiment. The duration ( $2\tau$ ) of the filter is chosen based on the different  $^1\text{H}$  spin-spin relaxation times of the headgroup and the glycerol protons.

a Tecmag pulse programmer and data acquisition system. The sample was spun using a Doty Scientific 7-mm spinner assembly installed in a home-built switching-angle spinning probehead described elsewhere (Eastman et al., 1992). The spinning speed was maintained between 1.6 and 2 kHz. The orientation of the rotor axis was controlled by a stepping motor attached to the bottom of the probe and a computerized motor controller with an angular precision of  $0.1^\circ$ . The proton radio frequency field strength was chosen between 30 and 40 kHz to avoid radio frequency heating of the sample. Carbon pulse lengths of about  $7\ \mu\text{s}$  were used.

2D heteronuclear correlation (HETCOR) spectra correlating the  $^{13}\text{C}$  and  $^1\text{H}$  chemical shifts in DMPC were obtained with the pulse sequence in Figure 2a (Hong et al., 1995b; Ernst et al., 1987; Lee & Griffin, 1989). A  $^1\text{H}$   $90^\circ$  pulse flips the  $^1\text{H}$  magnetization into the transverse plane, where it evolves under the  $^1\text{H}$  chemical shift interaction and the C–H scalar ( $J$ ) coupling during  $t_1$ . At the end of the evolution period, the  $^1\text{H}$  magnetization is transferred to the  $^{13}\text{C}$  spins by cross polarization (CP) (Pines et al., 1973), and the  $^{13}\text{C}$  magnetization is detected during  $t_2$ . The CP contact time was chosen to be 2 ms. Throughout the experiment, the sample is spun around an axis oriented at the magic angle,  $54.7^\circ$ , with respect to the external field in order to remove all anisotropic interactions. This leaves the  $^1\text{H}$  and  $^{13}\text{C}$  isotropic chemical shifts to be correlated in the 2D spectrum, with C–H  $J$ -splittings occurring in the  $^1\text{H}$  dimension. The peak intensities reflect the efficiencies of polarization transfer from the  $^1\text{H}$  to the  $^{13}\text{C}$  spins, which is a qualitative measure of the strengths of C–H dipolar couplings. The 99%  $^{13}\text{C}$  enrichment of the CO<sub>2</sub> carbon facilitates the observation of the resonances of those protons that have a significant coupling to the CO<sub>2</sub> carbon.

The assignment of the headgroup and the glycerol proton resonances in the CO<sub>2</sub> cross section of the 2D correlation spectrum is complicated by the partial overlap of the signals due to their similar isotropic chemical shifts. To separate these two types of  $^1\text{H}$  resonances, we inserted into the HETCOR sequence a relaxation filter (Figure 2b) that suppresses the signals of the glycerol protons based on their shorter spin–spin relaxation times ( $T_2$ ). The proton  $T_2$  filter consists of a delay  $2\tau$  with a  $180^\circ$  pulse at its center to refocus the chemical shift.

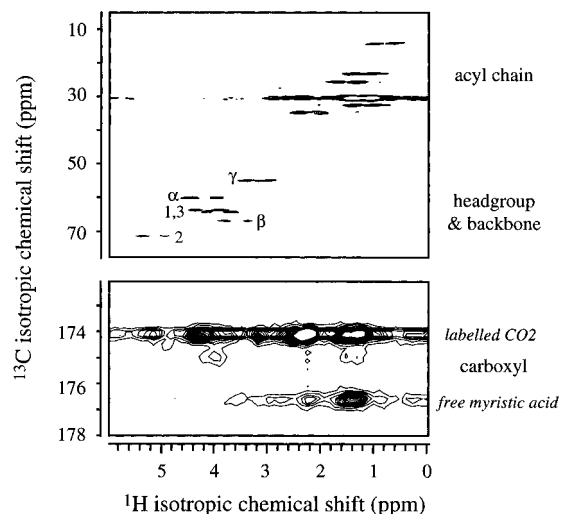


FIGURE 3: 2D  $^{13}\text{C}$ – $^1\text{H}$  chemical shift correlation spectrum of the CO<sub>2</sub>-labeled DMPC, obtained with the HETCOR sequence without the  $T_2$  filter. The CP contact time was 2 ms. (Top) Spectral region of the acyl chain and headgroup/glycerol segments. (Bottom) Spectral region of the carboxyl carbons. Multiple proton resonances are observed in the  $^{13}\text{C}$ CO<sub>2</sub> cross section at 174.2 ppm. They correspond to long-range dipolar couplings of the CO<sub>2</sub> carbon to various protons. The  $^{13}\text{C}$  resonance at 176.6 ppm results from the carboxyl carbon in the free myristic acid, which is present in the sample in small amounts. The measuring time was 7 h.

## RESULTS

Figure 3 presents the C–H chemical shift correlation spectrum of the  $^{13}\text{C}$ CO<sub>2</sub>-labeled DMPC. The acyl chain and the headgroup segments, whose  $^{13}\text{C}$  isotropic chemical shifts occur below 75 ppm, exhibit correlations only between the directly-bonded proton and carbon spins. Comparison with a one-dimensional (1D) proton MAS spectrum of the same sample (Figure 4d) demonstrates the higher resolution achieved by the separation in the carbon dimension. In particular, the headgroup and glycerol proton signals, which overlap strongly in the 1D spectrum, are distinguishable in the 2D spectrum. In the CO<sub>2</sub> carbon cross section at 174.2 ppm, intense signals can be observed at several proton chemical shifts (Figure 4a). The strongest signal, at 2.2 ppm, results from the acyl H<sub>2</sub> protons, which are the protons closest to the CO<sub>2</sub> carbon. Downfield, proton signals are observed at the chemical shifts of the H<sub>γ</sub> protons (3.3 ppm), the glycerol H<sub>G3</sub> protons or the headgroup H<sub>β</sub> protons (3.9 ppm), and the H<sub>G1</sub> protons or the H<sub>α</sub> protons (4.4 ppm). These multiple proton resonances reveal that the CO<sub>2</sub> carbon couples not only significantly to its nearest-neighbor protons but also to protons in the headgroup and glycerol backbone that are as far as 11 bonds away. Note that due to the lack of directly-bonded protons to the carboxyl carbon, C–H  $J$  splittings are not observed in the CO<sub>2</sub> cross section.

To distinguish between the overlapping signals of the headgroup and the glycerol protons, we exploited their different relaxation times. The H<sub>α</sub> and H<sub>β</sub> resonances are generally narrower than the glycerol H<sub>G1</sub> and H<sub>G3</sub> signals, indicating longer  $T_2$  relaxation times for the headgroup protons. This is verified by carbon CPMAS experiments in which a proton  $T_2$  filter of varying duration ( $2\tau$ ) is inserted before cross polarization. The resulting  $^{13}\text{C}$  spectra (Figure 5) show that at pre-echo delays of  $\tau \geq 100\ \mu\text{s}$ , the glycerol proton signals are sufficiently suppressed. Therefore, we chose an echo delay of  $\tau = 120\ \mu\text{s}$  for the  $T_2$ -filtered

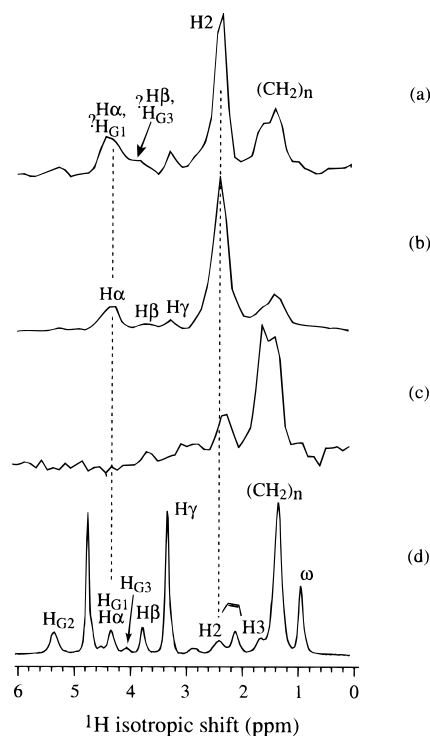


FIGURE 4: Cross sections of the CO<sub>2</sub> carbon (chemical shift = 174.2 ppm), obtained by the HETCOR experiment (a) without the  $T_2$  filter and (b) with the  $T_2$  filter. The duration of the  $T_2$  filter was  $2\tau = 240 \mu\text{s}$ . The coupling of the CO<sub>2</sub> carbon to all headgroup protons, particularly the H $\alpha$ 's, can be identified unambiguously. (c) Cross section of the carboxyl carbon in the free myristic acid (chemical shift = 176.6 ppm), obtained from the HETCOR spectrum in Figure 3. The H<sub>2</sub> intensity is reduced compared to (a) and (b), while the (CH<sub>2</sub>)<sub>n</sub> and H<sub>3</sub> intensities are significantly enhanced. (d) High-resolution <sup>1</sup>H MAS spectrum of DMPC for the assignment of <sup>1</sup>H chemical shifts.

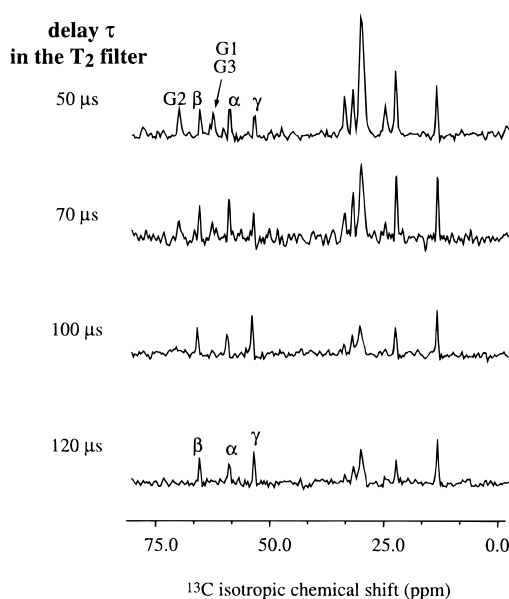


FIGURE 5: Carbon CPMAS spectra of DMPC, taken with a proton  $T_2$  filter of varying duration  $2\tau$ . The glycerol proton signals are suppressed at  $\tau \geq 100 \mu\text{s}$ . The CP contact time was 2 ms.

HETCOR experiment. The resulting CO<sub>2</sub> cross section is presented in Figure 4b. Clearly, the number and intensities of the proton signals between 3.5 and 5 ppm are substantially reduced. Only two peaks are significantly retained, and they can be unambiguously assigned to the H $\alpha$  (4.4 ppm) and

H $\beta$  (3.8 ppm) protons. The H $\alpha$  signal is particularly strong, indicating an appreciable CO<sub>2</sub>–H $\alpha$  coupling. In comparison, much weaker correlation signals are found for the H $\beta$  and H $\gamma$  protons. The difference in the peak intensities in the  $T_2$ -filtered spectrum also shows that spin diffusion among the headgroup protons is negligible, so they can be treated as independent groups of spins.

The cross section in Figure 4b also provides information on the conformation of the acyl chains. The pattern of the strong H<sub>2</sub> and the weak H<sub>3</sub> signals shows that the acyl chain is not in its all-trans conformation at the C2 segment. Otherwise the coupling of the CO<sub>2</sub> carbon to the H<sub>3</sub>'s would have been stronger than to the H<sub>2</sub>'s as a result of both distance and angular factors. The pattern expected for an acyl chain with mostly trans conformations is provided experimentally by the cross section at 176.7 ppm in the spectrum of Figure 3. It corresponds to the carboxyl carbon in free myristic acid, which is present in our system at a small concentration in an earlier batch of the sample. Figure 4c shows that the H<sub>3</sub> signal, in the region of the (CH<sub>2</sub>)<sub>n</sub> signals, is indeed more intense than the H<sub>2</sub> signal.

## DISCUSSION

The different proton resonance intensities between the CO<sub>2</sub> cross section of the  $T_2$ -filtered HETCOR spectrum and the 1D MAS spectrum provide valuable qualitative information on the relative strengths of the C–H dipolar couplings between the CO<sub>2</sub> carbon and various protons. The correlation between the CP signal intensity and the C–H dipolar coupling requires certain conditions. First, proton spin diffusion in the motionally-averaged phosphocholine bilayers must be negligible during the CP contact time, which is 2 ms in our experiments. The absence of significant spin diffusion between the headgroup and the glycerol protons during this CP contact time is proved by the bottom spectrum in Figure 5. If spin diffusion from the headgroup to the glycerol protons occurred, glycerol <sup>13</sup>C signals would be observed, which is clearly not the case. In addition, our previous <sup>1</sup>H WISE experiments with sample hopping confirm that little spin diffusion occurs even within 30 ms (Hong et al., 1995a). This is due to the fact that intramolecular H–H dipolar couplings are significantly weakened by the fast uniaxial motion of the lipid molecules around the director, while all intermolecular H–H and C–H dipolar couplings are averaged out by the rapid lateral diffusion of the molecules in the plane of the bilayer (Forbes et al., 1988; Hemminga & Cullis, 1982). Second, the CP contact time must be chosen within the initial increase of the CP transfer curve, so that the relative intensity of the CP signal compared to that from direct polarization corresponds to the strength of the C–H dipolar coupling. For the expected coupling strengths of 120 Hz and less, after 2 ms the CP transfer curve is still within the initial rise. In addition, it was verified experimentally that the 2 ms contact time indeed falls within the region of the initial monotonic rise of the CP efficiencies for all the CO<sub>2</sub>–H dipole pairs.

The strengths of the C–H dipolar couplings are related to the internuclear distances and orientations relative to the motional axis. Generally, the size of the motionally-averaged dipolar coupling is given by

$$\bar{\delta}_{\text{CH}} = -\frac{\mu_0}{4\pi} \hbar \gamma_{\text{C}} \gamma_{\text{H}} \left\langle \frac{1}{r_{\text{CH}}^3} \frac{1}{2} (3 \cos^2 \theta_{\text{CH}} - 1) \right\rangle$$

where  $r_{\text{CH}}$  is the internuclear distance and  $\theta_{\text{CH}}$  is the instantaneous angle between the C–H internuclear vector and the bilayer normal. Thus, the relatively strong CO2–H $\alpha$  coupling found here indicates that both the CO2–H $\alpha$  distance and the average orientation (relative to the director) of the CO2–H $\alpha$  vector must be favorable for producing a sizable C–H coupling. In other words, the CO2–H $\alpha$  distance is sufficiently small, and  $\theta_{\text{CH}}$  is close to 0°. This suggests that the H $\alpha$  protons are located directly above the CO2 carbon, if the director is taken to point up. In comparison, the H $\beta$  signal is much weaker than that of H $\alpha$ . A mobility difference can be ruled out as a full explanation for this, since the  $\alpha$  and  $\beta$  segments are directly bonded. Therefore, the difference between the H $\alpha$  and H $\beta$  intensities indicates that the H $\beta$ 's are on average more distant from the CO2 segment than the H $\alpha$ 's and/or that the H $\beta$ 's are not located directly above the *sn*-2 chain. Similarly, the low intensity of the H $\gamma$  signal, which is particularly remarkable because there are 4.5 times more H $\gamma$  protons than H $\alpha$  or H $\beta$  protons, can be attributed to their large distances from CO2, as well as to the additional degrees of rotational freedom of the methyl groups around the C $\beta$ –N and N–C $\gamma$  bonds.

The qualitative results on the couplings of the CO2 carbon to the headgroup protons can be used to test models of the phosphocholine headgroup orientation. For instance, in a molecular model derived from the joint refinement of X-ray and neutron scattering data (Wiener & White, 1992), the  $\alpha$  protons point up toward the bilayer surface. This is unlikely, in light of our dipolar coupling results, as the upward orientation would make the CO2–H $\alpha$  distance large and its coupling too weak to be observed.

The proximity between the CO2 carbon and the H $\alpha$  protons is consistent with the bend of the phosphocholine headgroup from the glycerol backbone toward the *sn*-2 chain and the bend of the beginning of the *sn*-2 chain toward the headgroup. These features are found in the folded conformation of molecule B in the crystal structure of DMPC (Figure 1) (Pearson & Pascher, 1979). The other conformation in the crystal, molecule A, exhibits larger distances between the CO2 carbon and the H $\alpha$ 's and an oblique orientation of the corresponding internuclear vectors with respect to the bilayer normal, which is taken to be along the molecular long axis. Both factors are unfavorable for producing a significant C–H coupling. Therefore, the relative strengths of the long-range C–H dipole couplings obtained from the HETCOR spectra show that a folded-back headgroup conformation, similar to molecule B in the crystal, is significantly populated in the liquid-crystalline bilayer. Without further analysis, this conclusion alone does not rule out the presence of other conformations in the crystal, since the dipole couplings would be reduced by the presence of type-A conformations, but could still be dominated by the strong coupling in the folded-back state.

Guided by the strong indication of a bent-back headgroup structure, we reexamined the dipolar couplings reported in the literature in an attempt to constrain the headgroup orientation in phosphocholine lipids. In particular, the  $^{31}\text{P}$ –

$^{13}\text{C}$  dipolar couplings involving the CO2 site (50 Hz) and the glycerol G3 site ( $240 \pm 20$  Hz) (Sanders 1993) are relatively large and serve as strong constraints. In our analysis, we consider for simplicity a single backbone conformation, which is sufficient to capture the essential features of type-A and type-B conformations. The overall wobbling of the molecule is taken into account by a molecular order parameter of 0.6 (Meier et al., 1986). For generality, instead of assuming a certain director orientation, we consider various orientations of the bilayer normal with respect to the G2–G3 bond. The analysis shows that the NMR couplings calculated for any conformation similar to molecule A are strongly inconsistent with the experimental data. The magnitude of the  $^{31}\text{P}$ –CO2 coupling would be smaller than 12 Hz, and that of the  $^{31}\text{P}$ –G3 coupling less than 160 Hz. This confirms our finding, based on the long-range CO2–H couplings, that structures with an extended headgroup similar to conformation A do not reproduce the NMR data.

In contrast, conformation B itself can yield  $^{31}\text{P}$ – $^{13}\text{C}$  couplings similar to (i.e., 0.4–1.3 times) the experimental values, depending on the exact choice of the direction of the bilayer normal. Although no choice of the bilayer normal in conformation B could reproduce all known NMR dipolar couplings for the glycerol backbone, a structure similar to conformation B but characterized by an even stronger bend of the headgroup (Figure 6) yields an acceptable solution. The existence of this structure, which will be discussed in more detail below, corroborates the predominance of type-B conformations with a bent-back headgroup in the phosphocholine bilayers.

So far the analysis has not quantified to what degree conformations of type-B dominate the structure of  $\text{L}_{\alpha}$ -DMPC. In order to estimate the relative populations of type-A and type-B conformations, it is necessary to determine whether a type-B structure can be found in which both  $^{31}\text{P}$ – $^{13}\text{C}$  ( $^{31}\text{P}$ –CO2 and  $^{31}\text{P}$ –G3) couplings exceed the experimental values significantly. If that were the case, contributions from type-A structures could be invoked to reduce the average couplings to the measured values. In our analysis, we find that due to the angle of about 40° between the  $^{31}\text{P}$ –CO2 and the  $^{31}\text{P}$ –G3 internuclear vectors, no structure exhibits large  $^{31}\text{P}$ – $^{13}\text{C}$  couplings for both sites. To generate a large  $^{31}\text{P}$ –G3 coupling, the phosphorus atom has to be set above the G3 carbon, which removes it to a larger distance and a more oblique angle from the CO2 carbon. The conformation with the largest combined  $^{31}\text{P}$ – $^{13}\text{C}$  couplings exhibits about 55 Hz and 280 Hz for the  $^{31}\text{P}$ –CO2 and  $^{31}\text{P}$ –G3 couplings, respectively. With an experimental value of  $50 \pm 8$  Hz for the  $^{31}\text{P}$ –CO2 coupling (Sanders, 1993), this allows for only 15% ( $\pm 15\%$ ) of conformation A. Thus, we conclude that structures similar to B, in which the  $\theta_1$  torsion is close to trans in order to make the headgroup bend back to the *sn*-2 chain, are the predominant conformations in the liquid-crystalline bilayer.

So far, we have mainly considered the overall structure of the molecule, distinguishing conformations of type-A and type-B. As outlined in the preceding paragraphs, by taking into account more and more NMR couplings from the literature, we are gradually led to a more and more specific molecular structure. This prompted us to test whether there is a single conformation for the “core” of the molecule, i.e., the glycerol backbone and the adjacent segments, that is

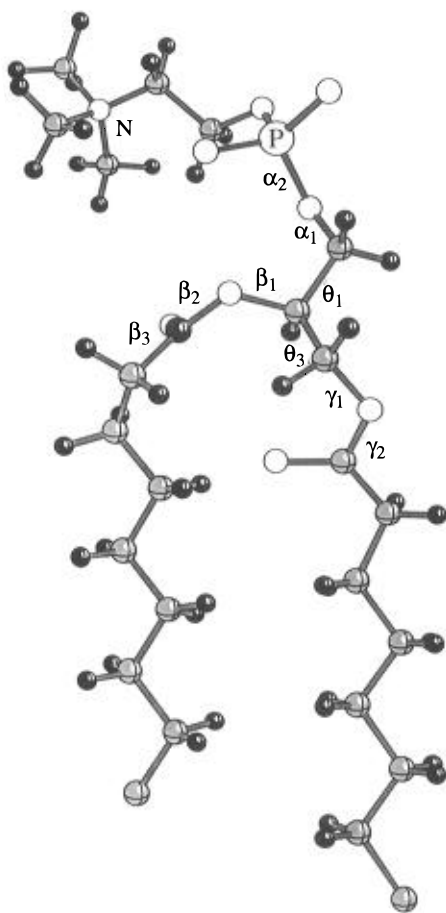


FIGURE 6: Structure of DMPC in the liquid-crystalline phase. It is consistent with 20 known NMR dipolar couplings ( $^{31}\text{P}$ – $^{13}\text{C}$ ,  $^{13}\text{C}$ – $^1\text{H}$ ,  $^1\text{H}$ – $^1\text{H}$ , and  $^{13}\text{C}$ – $^{13}\text{C}$  couplings) and chemical shift anisotropies ( $^{13}\text{COO}$  and  $^{31}\text{PO}_4$ ). A single backbone conformation is assumed. The bilayer normal forms an angle of  $35^\circ \pm 10^\circ$  with the G2–G3 bond and of  $109^\circ \pm 7^\circ$  with the G2–H<sub>G2</sub> bond. The phosphorus is positioned above the G2 carbon to fulfill the constraints of a large number of  $^{31}\text{P}$ – $^{13}\text{C}$  dipolar couplings. In contrast to the crystal structure, the  $\theta_3$  torsion ( $265^\circ$ ) is non-trans due to the markedly different C–H order parameters of the G1 and G3 segments. Torsion angles in the headgroup beyond the phosphate unit are not specified due to increased mobilities of the headgroup segments.

consistent with all known NMR data. We considered 20 anisotropic NMR couplings from the literature, in particular the  $^{31}\text{P}$ –G3,  $^{31}\text{P}$ –CO2,  $^{31}\text{P}$ –G2,  $^{31}\text{P}$ –G1, and  $^{31}\text{P}$ –CO1 (Sanders, 1993; Hong et al., 1995a); G3–H<sub>G3</sub> and G2–H<sub>G2</sub> (Gally et al., 1975; Strenk et al., 1985); and H<sub>G3</sub>–H<sub>G3</sub> (Hong et al., 1995a) dipolar couplings, and the chemical shift anisotropies of  $^{13}\text{CO}$  (Sanders, 1993; Braach-Maksvytis & Cornell, 1988) and  $^{31}\text{PO}_4$  (Griffin et al., 1978) segments. Again, the overall wobbling of the molecule was taken into account by a molecular order parameter of 0.6 (Meier et al., 1986).

A single conformation consistent with the NMR data was indeed found and is shown in Figure 6. At the central G2 site, the bilayer normal forms an angle of  $35^\circ \pm 10^\circ$  with the G2–G3 bond, and of  $109^\circ \pm 7^\circ$  with the G2–H<sub>G2</sub> bond, as determined by the G2–H<sub>G2</sub> order parameter (Strenk et al., 1985; Hong et al., 1995b). A parallel orientation of this molecular axis with the G2–G3 bond, commonly assumed in the literature (Seelig et al., 1977; Skarjune & Oldfield, 1979), can be excluded based on the fact that it does not allow for any  $^{31}\text{P}$ –G3 couplings larger than 160 Hz and yields too large a H<sub>G3</sub>–H<sub>G3</sub> coupling. The G1–G2–G3–O

torsion angle is trans ( $\theta_1 = 185^\circ$ ), producing a bent headgroup as in conformation B, while the O–G1–G2–G3 torsion is definitely not trans ( $\theta_3 = 265^\circ$ ), since the C–H bond order parameters for the G1 and G3 methylene groups are markedly different (Strenk et al., 1985). The G2–G3–O–P torsion angle ( $\alpha_1 = 110^\circ$ ), in conjunction with  $\theta_1$ , is crucial for positioning the phosphorus atom above the G2 site, in order to fulfill the constraints of the large number of  $^{31}\text{P}$ – $^{13}\text{C}$  couplings (Sanders, 1993; Hong et al., 1995a), especially those involving the CO2 and G3 carbons. The G3–O–P–O torsion ( $\alpha_2 = 170^\circ$ ) is less stringently defined than the  $\alpha_1$  torsion, as its only constraint is the  $^{31}\text{P}$  chemical shift anisotropy (Griffin et al., 1978; Seelig, 1978; Hauser et al., 1988). Although its trans conformation deviates from the X-ray structure (Pearson & Pascher, 1979), the bend of the headgroup is still maintained. As a consequence, the orientation of the  $\alpha$  segment is markedly different from that of most other methylene groups, as suggested by the positive sign of the C $\alpha$ –H $\alpha$  order parameters (Hong et al., 1995b). Further torsion angles in the headgroup ( $\alpha_3$ ,  $\alpha_4$ , and  $\alpha_5$ ) are not given here, because the consistently small order parameters of the C $\alpha$  and C $\beta$  segments indicate a high mobility, which makes a single-conformation description of the end of the headgroup inappropriate. In the acyl chain region, the structure of Figure 6 reproduces the measured chemical shift anisotropies for the CO1 (–9 ppm) and CO2 (0.5 ppm) carbons (Braach-Maksvytis & Cornell, 1988; Sander, 1993). The  $\beta_1$  and  $\beta_2$  torsions on the *sn*-2 chain are  $145^\circ$  and  $110^\circ$ , respectively, while the  $\gamma_1$  and  $\gamma_2$  torsions on the *sn*-1 chain assume gauche<sup>–</sup> ( $290^\circ$ ) and trans ( $180^\circ$ ) conformations. Further down the chains, the C2 and C2' methylene groups exhibit different orientations, since their C–H order parameters (Seelig & Seelig, 1975) and  $^{13}\text{C}$  chemical shift anisotropies (Sanders, 1993) differ substantially. The rest of the acyl chains is represented by trans conformations for convenience. A realistic structure, as characterized by the NMR order parameter profile, involves enhanced internal dynamics with an increasing number of gauche conformations toward the chain ends (Seelig & Seelig, 1974).

The rigid-backbone model presented here (Figure 6) successfully reproduces the NMR couplings in the core segments of the DMPC molecule in the liquid-crystalline state. Although it does not exclude a more complex structure with interchanging conformations, we believe that a single-conformation model, if it fits all known NMR data and correctly predicts other NMR couplings, provides a simple approximation to the structure that may be more valuable for further lipid research than more complicated multi-conformation models. In any case, the model can serve to visualize structural constraints imposed by the NMR couplings. From our measurement and analysis, we thus conclude that the L $\alpha$ -phase conformation of DMPC is dominated by one type of structure. It can be approximated by a rigid conformation in the core of the molecule and exhibits a bent-back headgroup.

## CONCLUSIONS

We have shown that two-dimensional NMR spectroscopy is a useful technique for obtaining structural information of mobile biomolecules such as phospholipids. By means of the chemical-shift correlation experiment, we obtained useful qualitative information on the relative strengths of long-range C–H dipolar couplings between the carboxyl carbon CO2

and the headgroup protons in DMPC. These data, together with long-range  $^{31}\text{P}$ – $^{13}\text{C}$  couplings from the literature, show that a folded-back headgroup conformation, in which the  $\text{H}\alpha$  protons are located above the  $\text{CO}_2$  carbon, is significantly populated in the liquid-crystalline bilayer. This bent-back headgroup is found in one of the two conformations, molecule B, of DMPC in the crystal. Taking into account 20 NMR anisotropic couplings from the literature, we propose a consistent molecular model for phosphocholine lipids in the liquid-crystalline state, with a rigid backbone in the core of the molecule, a bent-back headgroup, and increasing mobility toward the ends of the acyl chains and the headgroup.

## ACKNOWLEDGMENT

We thank Professor A. Pines for valuable discussions and support of this work.

## REFERENCES

- Braach-Maksyvytis, V. L. B., & Cornell, B. A. (1988) *Biophys. J.* 53, 839.
- Büldt, G., Gally, H. U., Seelig, J., & Zaccari, G. (1978) *Nature* 271, 182.
- Eastman, M. A., Grandinetti, P. J., Lee, Y. K., & Pines, A. (1992) *J. Magn. Reson* 98, 333.
- Ernst, R. R., Bodenhausen, G., & Wokaun, A. (1987) *Principles of Nuclear Magnetic Resonance in One and Two Dimensions*, Clarendon Press, Oxford.
- Forbes, J., Husted, C., & Oldfield, E. (1988) *J. Am. Chem. Soc.* 110, 1059.
- Gally, H. U., Niederberger, W., & Seelig, J. (1975) *Biochemistry* 16, 3647.
- Griffin, R. G., Powers, L., & Pershan, P. S. (1978) *Biochemistry* 17, 2718.
- Hauser, H., Radloff, C., Ernst, R. R., Sundell, S., & Pascher, I. (1988) *J. Am. Chem. Soc.* 110, 1054.
- Hemminga, M. A., & Cullis, P. R. (1982) *J. Magn. Reson.* 47, 307.
- Hermetter, A., & Paltauf, F. (1981) *Chem. Phys. Lipids* 28, 111.
- Hong, M., Schmidt-Rohr, K., & Nanz, D. (1995a) *Biophys. J.* 69, 1939.
- Hong, M., Schmidt-Rohr, K., & Pines, A. (1995b) *J. Am. Chem. Soc.* 117, 3310.
- Konstant, P. H., Pearce, L. L., & Harvey, S. C. (1994) *Biophys. J.* 67, 713.
- Lee, C. W. B., & Griffin, R. G. (1989) *Biophys. J.* 55, 355.
- Lehninger, A. L., Nelson, D. L., & Cox, M. M. (1993) *Principles of Biochemistry*, Worth Publishers, New York.
- Meier, P., Ohmes, E., & Kothe, G. (1986) *J. Chem. Phys.* 85, 3598.
- Pearson, R. H., & Pascher, I. (1979) *Nature* 281, 499.
- Petty, H. R. (1993) *Molecular biology of membranes: structure and function*, Plenum, New York.
- Pines, A., Gibby, M. G., & Waugh, J. S. (1973) *J. Chem. Phys.* 59, 569.
- Radhakrishnan, R., Robson, R. J., Takogaki, Y., & Khorana, H. G. (1981) *Methods Enzymol.* 72, 408.
- Salinger, Z., & Lapidot, Y. (1966) *J. Lipid Res.* 7, 174.
- Sanders, C. R. (1993) *Biophys. J.* 64, 171.
- Schmidt-Rohr, K., & Hong, M. (1995) *J. Phys. Chem.* 100, 3861.
- Seelig, A., & Seelig, J. (1974) *Biochemistry* 13, 4839.
- Seelig, A., & Seelig, J. (1975) *Biochim. Biophys. Acta* 406, 1.
- Seelig, J. (1978) *Biochim. Biophys. Acta* 515, 105.
- Seelig, J., & Seelig, A. (1980) *Q. Rev. Biophys.* 13, 19.
- Seelig, J., Gally, H.-U., & Wohlgemuth, R. (1977) *Biochim. Biophys. Acta* 467, 109.
- Silver, B. L. (1985) *The physical chemistry of membranes: an introduction to the structure and dynamics of biological membranes*, Solomon Press, Jamaica, NY.
- Skarjune, R., & Oldfield, E. (1979) *Biochemistry* 18, 5903.
- Stouch, T. R. (1993) *Mol. Simul.* 10, 335.
- Strenk, L. M., Westerman, P. W., & Doane, J. W. (1985) *Biophys. J.* 48, 765.
- Wiener, M. C., & White, S. H. (1992) *Biophys. J.* 61, 434.

BI953083I